

Preparation and properties of porous silicon carbide ceramics through coat-mix and composite additives process

ZHAO Hong-sheng, LIU Zhong-guo, YANG Yang, LIU Xiao-xue, ZHANG Kai-hong, LI Zi-qiang

Institute of Nuclear and New Energy Technology, Tsinghua University, Beijing 100084, China

Received 18 October 2010; accepted 29 November 2010

Abstract: The core-shell structure silicon-resin precursor powders were synthesized through coat-mix process and addition of $\text{Al}_2\text{O}_3\text{-SiO}_2\text{-Y}_2\text{O}_3$ composite additives. A series of porous silicon carbide ceramics were produced after molding, carbonization and sintering. The phase, morphology, porosity, thermal conductivity, thermal expansion coefficient, and thermal shock resistance were analyzed. The results show that porous silicon carbide ceramics can be produced at low temperature. The grain size of porous silicon carbide ceramic is small, and the thermal conductivity is enhanced significantly. Composite additives also improve the thermal shock resistance of porous ceramics. The bending strength loss rate after 30 times of thermal shock test of the porous ceramics which were added $\text{Al}_2\text{O}_3\text{-SiO}_2\text{-Y}_2\text{O}_3$ and sintered at 1650 °C is only 6.5%. Moreover, the pore inside of the sample is smooth, and the pore size distribution is uniform. Composite additives make little effect on the thermal expansion coefficient of the porous silicon carbide ceramics.

Key words: silicon carbide; porous ceramic; coat-mix; composite additives

1 Introduction

Porous silicon carbide ceramics are important materials, which exhibit lots of excellent properties of both porous ceramics and silicon carbide. Due to possessing a set of attractive properties, porous silicon carbide ceramics have been widely employed in many application fields, involving aerospace, energy, machinery, metallurgy, chemistry, environmental, biological and medical fields, using as filters, membranes, heat exchangers, thermal insulators, capacitors, sound-absorbing material, damping buffers, various sensors, catalysts and catalyst carriers, etc [1–3]. Porous silicon carbide ceramics have been synthesized using various methods [4], including oxidation bonding method [5], combustion synthesis, chemical vapor reaction, sol-gel [6] and carbothermal reduction reaction [7–8], preceramic foam processing [9], and coat-mix method. Coat-mix method has an extensive application prospect due to the advantages of simple technology, energy saving, high efficiency, controllable process and environmental compatibility. The product of coat-mix technology possesses controllable pore size, narrow pore

size distribution and high purity [10–11]. Researches show that the porosity, strength and thermal shock resistance of porous silicon carbide ceramics could be improved by adding sintering additives such as Al_2O_3 , Y_2O_3 , MgO , K_2O and SiO_2 [12–13].

In this work, the silicon-resin precursor powders with core-shell structure were synthesized through coat-mix process, and Al_2O_3 , $\text{Al}_2\text{O}_3\text{-SiO}_2$ and $\text{Al}_2\text{O}_3\text{-SiO}_2\text{-Y}_2\text{O}_3$ were introduced as sintering additives, respectively. Then porous silicon carbide ceramics were produced after molding, carbonization and sintering. The phase, surface morphology, porosity, thermal conductivity, thermal expansion coefficient, bending strength and thermal shock resistance of porous silicon carbide ceramics were analyzed.

2 Experimental

2.1 Sample preparation

The silicon-resin precursor powders with core-shell structure were synthesized through coat-mix process from industrial grade silicon powder and barium phenolic resin. Additives were chemically pure neutral Al_2O_3 with particle size of 75–150 μm , chemically pure

Y₂O₃ and analytically pure SiO₂, respectively. Taking the total mass of precursor powders of 100 g, the sample batch and sintering temperature of porous silicon carbide ceramics are shown in Table 1.

Table 1 Batch and sintering temperature of porous silicon carbide ceramics

Sample No.	<i>m</i> (Powder)/g	<i>m</i> (Al ₂ O ₃)/g	<i>m</i> (SiO ₂)/g	<i>m</i> (Y ₂ O ₃)/g	Temperature/°C
S1	100	3	1	0.71	1 450
S2	100	3	1	0.71	1 550
S3	100	3	1	0.71	1 650
S4	100	3	1	0.71	1 750
S5	100	0	0	0	1 650
S6	100	3	0	0	1 650
S7	100	3	1	0	1 650

After mixing, the precursor powder and additives were pressure molded at 50–140 °C and 0.5–50 MPa for 20–120 min. Then the materials were carbonized at 600–1 000 °C for 1–4 h under argon atmosphere. After that the samples were treated by high temperature vacuum sintering at 1 450–1 750 °C for 2 h, with heating rate of 5–10 °C/min.

2.2 Characterization of samples

The morphology and phase of porous silicon carbide ceramics were analyzed by S-3000N type scanning electron microscope and Bruker P4 type X-ray diffraction instrument, respectively. The porosity of the sample was measured by Autopore IV 9510 mercury porosimeter. LFA-427 type laser flash apparatus, DIL-402C type thermal dilatometer and STA-449 type simultaneous thermal analyzer were used to measure the thermal diffusivity (α), linear expansion coefficient and specific heat capacity (c_p). The density of the sample was obtained through drainage method, and the thermal conductivity was calculated using the formula $\lambda = \alpha \rho c_p$.

The products were processed to be samples of 3 mm×4 mm×40 mm by diamond surface grinding machine. Then three-point bending strength measurement of 30 mm span was taken on the samples by Zwickz005 type material detection equipment. The samples were heated to 800 °C and heat shock 30 times under air atmosphere. Thermal shock resistance was performed by bending strength loss rate of materials [14]:

$$\eta = \frac{\sigma_0 - \sigma_1}{\sigma_0} \times 100\% \quad (1)$$

where η is bending strength loss rate; σ_0 is bending strength before thermal shock; σ_1 is bending strength after thermal shock.

3 Results and discussion

3.1 Effect of sintering temperature

Figure 1 shows the XRD patterns of porous silicon carbide ceramics with Al₂O₃-SiO₂-Y₂O₃ additives at different sintering temperatures. In Fig. 1, the peaks at $2\theta = 36^\circ, 41^\circ, 60^\circ, 72^\circ$ and 76° are assigned to (1 1 1), (2 0 0), (2 2 0), (3 1 1) and (2 2 2) planes of cubic SiC according to the standard JCPDS cards (29-1129). It is found that no carbon peaks and silicon peaks can be observed in these patterns. The pattern of sample S1 shows that only β -SiC diffraction peaks appear at the sintering temperature of 1 450 °C. It is indicated that SiC ceramic is already obtained at 1 450 °C. Figure 2 shows the surface SEM images of the samples sintered at different temperatures. It can be seen from Fig. 2 that the microstructure of sample S1 is uniform and dense, indicating that the composite additives decrease the formation temperature of porous silicon ceramics.

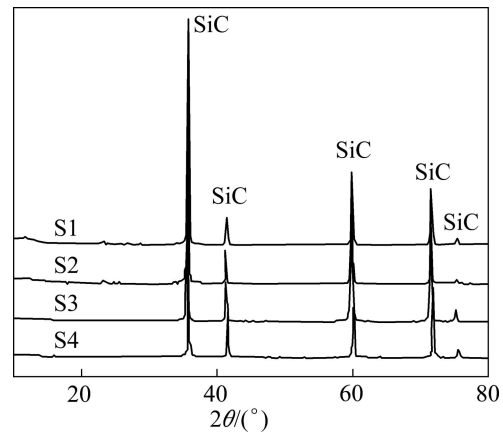


Fig. 1 XRD patterns of porous silicon carbide ceramics at different sintering temperatures

Figure 3 shows the bending strength and bending strength loss rate of samples, which were taken Al₂O₃-SiO₂-Y₂O₃ as additive, and sintered at different temperatures. It can be seen from the curves that the bending strengths of all the samples before and after thermal shock gradually decrease along with increasing the sintering temperature from 1 450 °C up to 1 650 °C. While the strength of the samples before and after thermal shock decreases rapidly from 1 650 °C to 1 750 °C. The bending strength loss rate of the sample sintered at 1 650 °C (S3) is only 6.5%, which is the lowest among all samples. When the temperature is below 1 650 °C, the bending strength loss rate of the samples gradually decreases as the sintering temperature increases. The bending strength loss rate of the sample sintered at 1 750 °C (S4) reaches 52.8%. The results show that the high

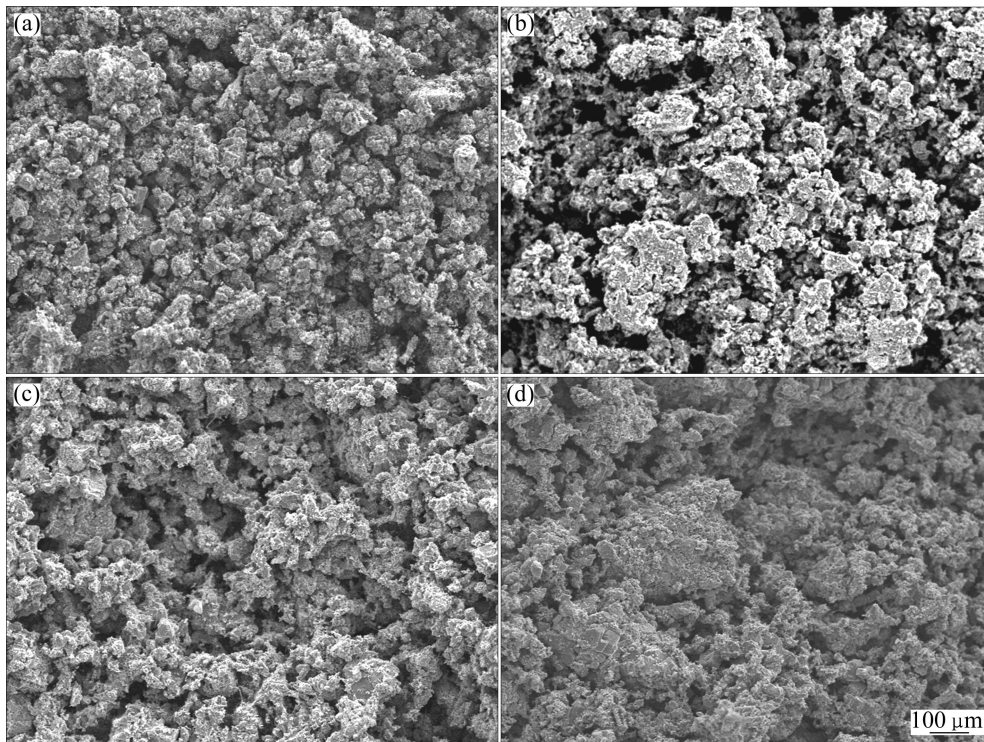


Fig. 2 Surface SEM images of porous silicon carbide ceramics at different sintering temperatures: (a) S1; (b) S2; (c) S3; (d) S4

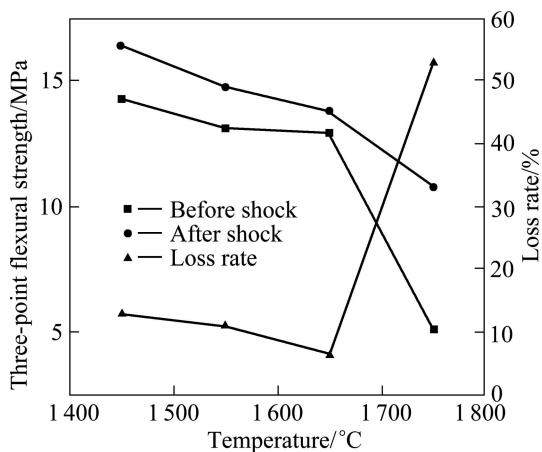


Fig. 3 Thermal shock resistance of porous silicon carbide ceramics sintered at different temperatures

sintering temperature would lead to the decrease of the thermal shock resistance.

Figure 4 shows the effect of sintering temperature on the thermal conductivity of the samples. The results show that the sample sintered at 1 650 °C has the highest thermal conductivity. It is corresponding to the data of the bending strength before and after thermal shock at 1 650 °C (Fig. 3).

Figure 5 shows the effect of sintering temperature on the linear expansion coefficient (α) of porous silicon carbide. As shown in Fig. 5, the sintering temperature has no obvious influence on linear expansion of samples. The linear expansion coefficient of the sample S1

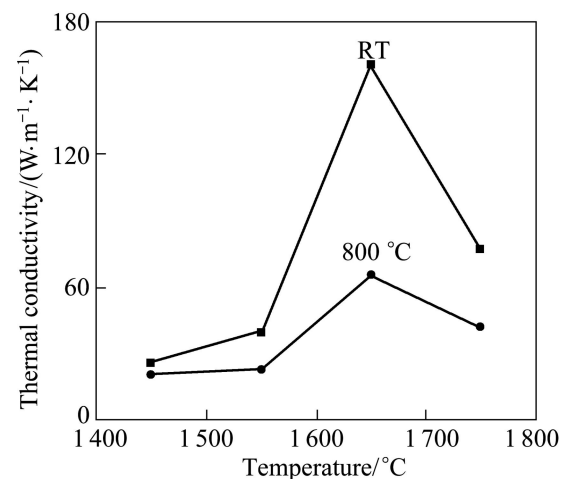


Fig. 4 Thermal conductivity at RT and 800 °C for porous silicon carbide ceramics sintered at different temperatures

sintered at 1 450 °C is lower at the low temperatures. While the linear expansion coefficient of sample S3 sintered at 1 650 °C is higher at the high temperatures.

Figure 6 shows the effect of sintering temperature on porosity of the samples. As shown in Fig. 6, the bending strength and thermal shock resistance of sample S3 are very good, and the porosity of sample S3 is the highest. From the surface morphology of sample S3 shown in Fig. 2, it can be seen that sample S3 has uniform pore size distribution, which can disperse thermal elastic strain energy. Besides, sample S3 has smooth pore wall, which can relax the stress. Therefore,

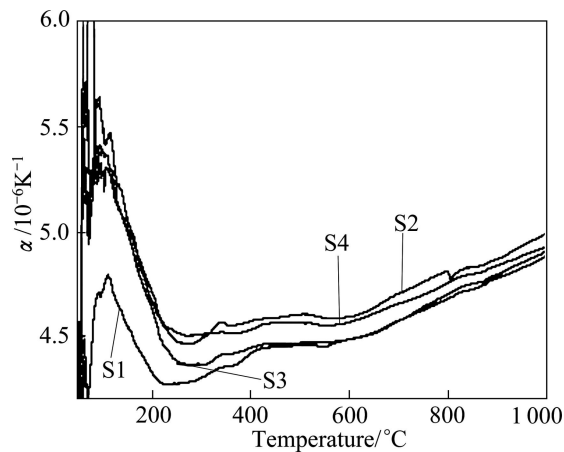


Fig. 5 Thermal expansion coefficient of porous silicon carbide ceramics sintered at different temperatures

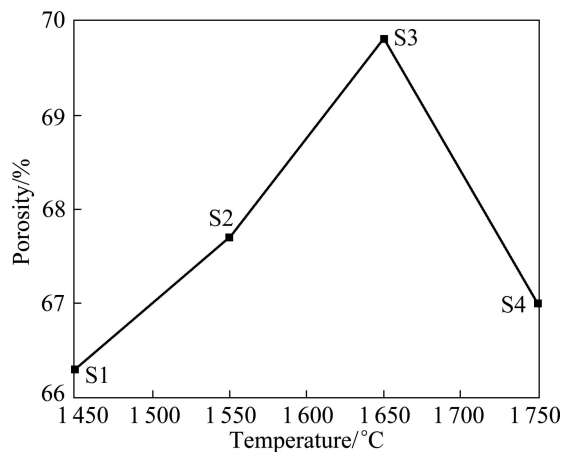


Fig. 6 Porosity of porous silicon carbide ceramics sintered at different temperatures

the thermal shock resistance of sample S3 is improved.

3.2 Effect of different additives

The bending strength and bending strength loss rate of porous silicon carbide ceramics with different additives before and after thermal shock at 800 °C are shown in Table 2.

As shown in Table 2, sample S3 ($\text{Al}_2\text{O}_3\text{-SiO}_2\text{-Y}_2\text{O}_3$ as the composite additive, sintered at 1650 °C) has the

Table 2 Thermal shock resistance of porous silicon carbide ceramics with different additives

Sample No.	Thermal shock resistance/MPa		Loss rate/%
	Before thermal shock	After thermal shock	
S3	13.8	12.9	6.5
S5	11.1	3.8	65.8
S6	1.9	1	47.4
S7	9.1	3.7	59.3

highest bending strength both before and after the thermal shock. Besides, the bending strength loss rate of sample S3 after thermal shock is the lowest, and far lower than those of samples with other additives. As shown in XRD patterns (see Fig. 7), both samples S3 and S7 with composite additives perform the peaks of mullite phase ($3\text{Al}_2\text{O}_3\cdot 2\text{SiO}_2$), which has better thermal shock resistance and mechanical characteristics [15].

As shown in Fig. 7, sample S3 has more mullite phases because of the addition of Y_2O_3 , which may promote liquid phase sintering and then result in more mullite phases. It also can be found that the additives of the other two compounds reduce the bending strength before thermal shock. Particularly, the bending strength of sample S6 obtained by adding Al_2O_3 before thermal shock is only 1.9 MPa, which is far lower than that of other samples.

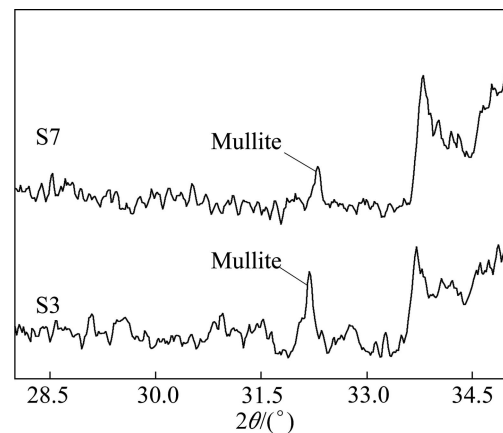


Fig. 7 XRD patterns of samples S3 and S7

Therefore, the formation of mullite phase is beneficial to enhance the bending strength before thermal shock and thermal shock resistance of porous silicon carbide ceramics. The addition of Y_2O_3 decreases the formation temperature of mullite, while the liquid phase sintering makes the grain refinement. Table 3 exhibits the effect of additives on the thermal conductivity of the porous silicon carbide ceramics. As shown in Table 3, $\text{Al}_2\text{O}_3\text{-SiO}_2\text{-Y}_2\text{O}_3$ composite additive increases the thermal conductivity obviously. It is ascribed to the second phase mullite distributed continuously around matrix grains in this system, while no continuous distribution of mullite phase appeared for the samples with the other two additives. As shown in Table 4, porous silicon carbide products keep the characteristics of high porosity after composite additives. The sample S3 ($\text{Al}_2\text{O}_3\text{-SiO}_2\text{-Y}_2\text{O}_3$ as additive), which has the best thermal shock resistance, remains nearly 70% porosity. The sample with $\text{Al}_2\text{O}_3\text{-SiO}_2$ additive has higher porosity, but its bending strength and thermal shock resistance are not ideal.

Table 3 Thermal conductivity of porous silicon carbide ceramics with different additives

Sample No.	Thermal conductivity/(W·m ⁻¹ ·K ⁻¹)	
	Room temperature	800 °C
S5	43	21
S6	30	17
S7	38	14
S3	160	65

Table 4 Porosity of porous silicon carbide ceramics with different additives

Sample No.	Porosity/%
S5	67.9
S6	65.0
S7	73.7
S3	69.8

Figure 8 shows the thermal expansion coefficient of samples with different additives and sintered at different temperatures. At low temperature, the sample with Al₂O₃-SiO₂-Y₂O₃ composite additive has the lowest linear expansion coefficient, while the sample with Al₂O₃-SiO₂ composite additive has the lowest linear expansion coefficient at high temperature. Whereas, as shown in Fig. 8, composite additives make no remarkable influence on linear expansion coefficient of ceramics.

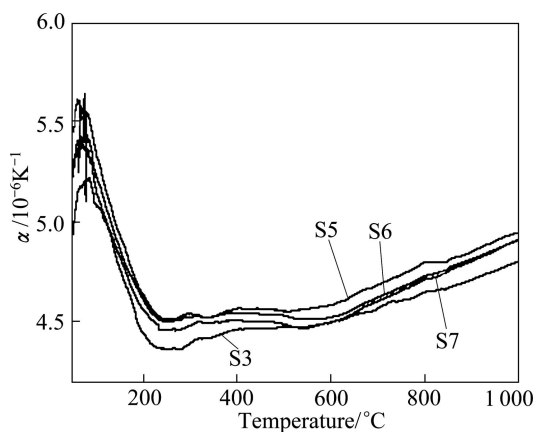
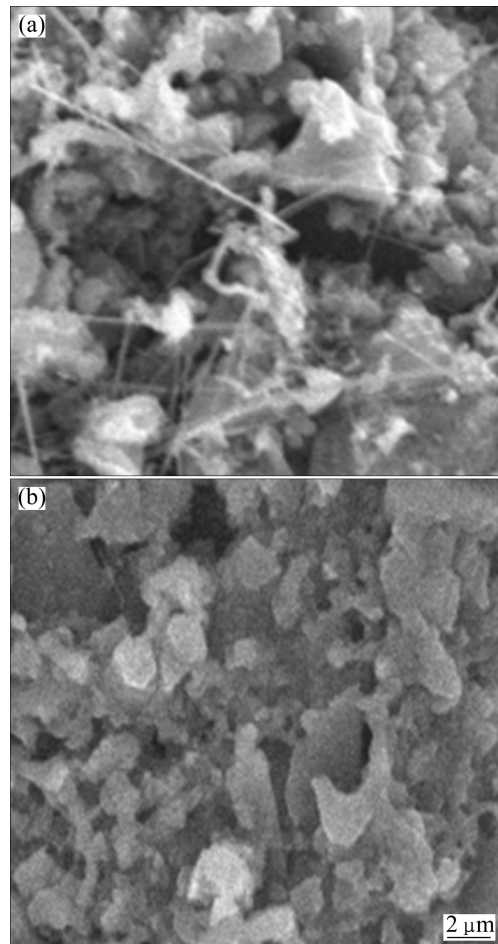
**Fig. 8** Thermal expansion coefficient of porous silicon carbide ceramics with different additives

Figure 9 shows the SEM images of porous silicon carbide ceramics without additive and with Al₂O₃-SiO₂-Y₂O₃ additives. As shown in Fig. 9, the grains of samples with Al₂O₃-SiO₂-Y₂O₃ additives are refined. Fine-grained materials generally have better strength and thermal stress resistance than coarse grain. Therefore, the thermal shock resistance of porous

**Fig. 9** SEM images of porous silicon carbide ceramics: (a) Without additives (S5); (b) With Al₂O₃-SiO₂-Y₂O₃ additive (S3)

silicon carbide ceramics with Al₂O₃-SiO₂-Y₂O₃ additive is enhanced.

4 Conclusions

1) Based on the fabrication of core-shell structure silicon-resin precursor powders by coat-mix method, porous silicon carbide ceramics were prepared at lower temperature by adding a small amount of Al₂O₃-SiO₂-Y₂O₃.

2) By adding Al₂O₃-SiO₂-Y₂O₃, more mullite phases in the porous silicon carbide ceramics generate, the silicon carbide grains are refined, and the wall of the pores becomes smoother.

3) Porous silicon carbide ceramics synthesized through composite additive have high porosity; both the thermal shock resistance and the thermal conductivity are enhanced. While the composite additive performs less impact on the linear expansion coefficient of the samples.

4) Porous silicon carbide ceramics with the highest thermal conductivity, the highest porosity, and the best thermal shock resistance were synthesized by adding a proper amount of $\text{Al}_2\text{O}_3\text{-SiO}_2\text{-Y}_2\text{O}_3$ and sintering at $1\ 650\ ^\circ\text{C}$.

References

- [1] MOENE R, MAKKEE M, MOULIJN J A. High surface area silicon carbide as catalyst support characterization and stability [J]. *Applied Catalysis A*, 1998, 167(2): 321–330.
- [2] MIMURA H, MATSUMOTO T, KANEMITSU Y. Light emitting devices using porous silicon and porous silicon carbide [J]. *Solid-State Electronics*, 1996, 40: 501–504.
- [3] CIORA R J, FAYYAZ B, LIU P K T, SUWANMETHANOND V, MALLADA R, SAHIMI M, TSOTSIS T T. Preparation and reactive applications of nanoporous silicon carbide membranes [J]. *Chemical Engineering Science*, 2004, 59: 4957–4965.
- [4] ZHANG Lin, QU Xuan-hui, DUAN Bo-hua, HE Xin-bo. Progress in research on porous silicon carbide [J]. *Powder Metallurgy Technology*, 2007, 25(2): 139–144. (in Chinese)
- [5] SHE J H, YANG J F, KONDO N, OHJI T, KANZAKI S, DENG Z Y. High-strength porous silicon carbide ceramics by an oxidation-bonding technique [J]. *Journal of the American Ceramic Society*, 2002, 85(11): 2852–2854.
- [6] VERDENELL I M, PAAROLA S, CHASSAGNEUX F, LETOFFE J M, VINCENT H, SCHARFF J P, BOUIX J. Sol-gel preparation and thermo-mechanical properties of porous $x\text{Al}_2\text{O}_3\text{-}y\text{SiO}_2$ coatings on SiC Hi-Nicalon fibres [J]. *Journal of the European Ceramic Society*, 2003, 23(8): 1207–1213.
- [7] EOM J H, KIM Y W, SONG I H, Kim H D. Microstructure and properties of porous silicon carbide ceramics fabricated by carbothermal reduction and subsequent sintering process [J]. *Materials Science and Engineering A*, 2007, 464: 129–134.
- [8] QIAN J M, WANGJ P, QIAO GJ, JIN Z H. Preparation of porous SiC ceramic with a woodlike microstructure by sol-gel and carbothermal reduction processing [J]. *Journal of the European Ceramic Society*, 2004, 24(10–11): 3251–3259.
- [9] WANG C, WANG J, PARK C B, KIM Y W. Cross-linking behavior of a polysiloxane in preceramic foam processing [J]. *Journal of Materials Science*, 2004, 39(15): 4913–4915.
- [10] SHI L M, ZHAO H S, YAN Y H, TANG C H. Fabrication of high purity porous SiC ceramics using coat mix process [J]. *Materials Science and Engineering A*, 2007, 460: 645–647.
- [11] SHI L M, ZHAO H S, YAN Y H, LI Z Q, TANG C H. High specific surface area porous SiC ceramics coated with reticulated amorphous SiC nanowires [J]. *Physica E*, 2008, 40: 2540–2544.
- [12] DING S Q, ZENG Y P, JIANG D L. In-situ reaction bonding of porous SiC ceramics [J]. *Materials Characterization*, 2008, 59: 140–143.
- [13] DING S Q, ZENG Y P, JIANG D L. Thermal shock behaviour of mullite-bonded porous silicon carbide ceramics with yttria addition [J]. *Journal of Physics D*, 2007, 40: 2138–2142.
- [14] JIA De-chang, SONG Gui-ming. Properties of inorganic nonmetal materials [M]. Beijing: Science Press, 2008. (in Chinese)
- [15] LIN Y, TSANG C. Fabrication of mullite/SiC and mullite/zirconia/SiC composites by ‘dual’ in-situ reaction syntheses [J]. *Materials Science and Engineering A*, 2003, 344: 168–174.

基于包混和复合添加工艺的多孔碳化硅陶瓷的制备和性能

赵宏生, 刘中国, 杨阳, 刘小雪, 张凯红, 李自强

清华大学 核能与新能源技术研究院, 北京 100084

摘要: 采用包混工艺合成核-壳结构的硅-树脂先驱体粉体, 引入 $\text{Al}_2\text{O}_3\text{-SiO}_2\text{-Y}_2\text{O}_3$ 复合添加剂, 通过成型、炭化和烧结工艺制备多孔碳化硅陶瓷。分析多孔碳化硅陶瓷样品的物相、形貌、孔隙率、热导率、热膨胀系数和抗热震性能。结果表明: 复合添加能够在较低的温度下制得多孔碳化硅陶瓷; 陶瓷样品的晶粒较小, 明显增强了多孔碳化硅陶瓷的导热性能; 复合添加提高了碳化硅陶瓷的抗热震性能, 添加 $\text{Al}_2\text{O}_3\text{-SiO}_2\text{-Y}_2\text{O}_3$ 并且在 $1\ 650\ ^\circ\text{C}$ 下烧结制备的多孔碳化硅陶瓷经过30次热震后的抗弯强度损失率为6.5%; 陶瓷样品的孔壁更加光滑, 孔分布更均匀; 复合添加对多孔碳化硅陶瓷热膨胀系数的影响较小。

关键词: 碳化硅; 多孔陶瓷; 包混; 复合添加剂

(Edited by LI Xiang-qun)